Breakdown of Langmuir Adsorption Isotherm in Small Closed Systems

Ronen Zangi[*,1,2,3]

[1] *Donostia International Physics Center (DIPC), 20018 Donostia-San Sebastián, Spain*

[2] *Department of Organic Chemistry I, University of the Basque Country UPV/EHU, 20018 Donostia-San Sebastián, Spain*

[3] *IKERBASQUE, Basque Foundation for Science, 48009 Bilbao, Spain*

November 29, 2023

---

[*]r.zangi@ikerbasque.org

Abstract

For more than a century, monolayer adsorptions in which adsorbate molecules and adsorbing sites behave ideally have been successfully described by Langmuir adsorption isotherm. For example, the amount of adsorbed material, as a function of concentration of the material which is not adsorbed, obeys Langmuir's equation. In this paper we argue this relation is valid only for macroscopic (large enough) systems. However, when particle numbers of adsorbate molecules and/or adsorbing sites are small, Langmuir's model fails to describe the chemical equilibrium of the system. This is because the kinetics of forming, or the probability of observing, occupied sites arises from two-body interactions, and as such, ought to include cross-correlations between particle numbers of the adsorbate and adsorbing sites. The effect of these correlations, as reflected by deviations in predicting composition when correlations are ignored, increases with decreasing particle numbers and becomes substantial when only few adsorbate molecules, or adsorbing sites, are present in the system. In addition, any change that augments the fraction of occupied sites at equilibrium (e.g., smaller volume, lower temperature, or stronger adsorption energy) further increases the discrepancy between observed properties of small systems and those predicted by Langmuir's theory. In contrast, for large systems these cross-correlations become negligible, and therefore when expressing properties involving two-body processes, it is possible to consider independently the concentration of each component. By applying statistical mechanics concepts, we derive a general expression of the equilibrium constant for adsorption. It is also demonstrated that in ensembles in which total numbers of particles are fixed, the magnitudes of fluctuations in particle numbers alone, can predict the average chemical composition of the system. Moreover an alternative adsorption equation, predicting the average fraction of occupied sites from the value of the equilibrium constant, is proposed. All derived relations and predictions were tested against results obtained by Monte Carlo simulations.

Introduction

Adsorption, the process in which molecules A, say in a gas phase, adsorb onto sites S (here taken with single occupancy) of a, e.g. solid, surface can be described by the following chemical equation,

$$A(g) + S \rightleftharpoons SA \qquad . \tag{1}$$

Assuming ideal behavior of all components, which also implies no multilayer formation, the equilibrium properties of the system, such as average fraction of occupied sites $\langle \theta_{SA} \rangle$, are well described by the celebrated Langmuir adsorption isotherm[1],

$$\langle \theta_{SA} \rangle = \frac{K \langle c_A \rangle}{c^{\varnothing} + K \langle c_A \rangle} \qquad , \tag{2}$$

where $\langle c_A \rangle$ is average concentration of gas particles at equilibrium, K, the equilibrium (Langmuir) constant of the reaction, and $c^{\varnothing}$, the standard (reference) concentration of adsorbate gas, introduced here to comply with the convention of rendering K unitless. Although the adsorption process in Eq. 1 is chosen to take place from a gaseous to a solid phase, a corresponding adsorption process of solutes from solution onto an interface formed at contact with solid, liquid, or gas phases yields the same Langmuir equation (Eq. 2). It should be pointed out that in case the adsorbate molecules are dissolved in a liquid, the change in adsorbate-solvent interactions upon adsorption is accounted for by an effective adsorption energy[2]. A vast number of studies, encompassing different scientific fields, confirm that systems adhering to assumptions mentioned above do obey the Langmuir equation[3–20], whereas non-ideal systems, for example those characterized by substantial interactions between the adsorbed molecules, exhibit certain degree of deviations[21]. In practice, to examine compliance with Langmuir's isotherm, experiments with different amounts of adsorbate A are performed where its unadsorbed concentration and amount adsorbed, both at equilibrium, are measured. Then, these measured data points are fitted to the relation in Eq. 2, either in its non-linear or in one of its linear forms[22–24], aiming to extract the value of K, and sometimes, the total number of adsorbing sites, $N_S^{\text{total}} = \langle N_{SA} \rangle / \langle \theta_{SA} \rangle$. Note, none of the assumptions made in deriving Langmuir equation[1,25] imposes conditions on the size of the system, or alternatively, on

the particle numbers of the adsorbate and/or adsorbing sites. Thus, Eq. 2 is implied to be valid for any system size, also for those composed of only few A molecules or only few S sites.

Yet, Polak and Rubinovich argued that adsorption under nanoconfinement exhibit equilibrium properties deviating from those predicted by Langmuir's model due to an entropic effect[26] and Ramaswamy et al. argued that rate equations are qualitatively incorrect in sub-critical volumes[27]. Furthermore, single-molecule experiments of small-sized systems undergoing association reactions (where both reactants are mobile in space) find that concentrations of bound complexes do not agree with predictions of the conventional chemical equilibrium theory[28–37]. Similar behavior was also reported by computational studies[38–53]. In light of these findings, we recently demonstrated that for bimolecular reactions, averages of quantities observed at small (finite) systems are different than those observed at large or macroscopic system[54–56]. This inhomogeneous function behavior of system's properties is applicable for closed systems, that is for systems in which the total numbers of particles are fixed, such as the canonical ensemble. Then by definition, as time or configurations are propagated, the particle numbers of all components are subject to fluctuations with relative magnitudes that increase as system's size decreases. In fact, from the magnitudes of these fluctuations alone it is possible to determine average properties of the system including the number (or concentration) of bound particles.

What is then the difference between small and large systems? Because we are dealing with bimolecular reactions, which necessarily proceed via two-body interactions, cross-correlations in particle numbers (or concentrations) must be taken into account when describing mass-actions at equilibrium[54–57]. The importance of these cross-correlations are augmented as particle numbers and/or volume decrease, as well as, for lower temperatures or larger binding energies, and the amplitude of their effect can reach few orders of magnitudes. On the other hand, when the system is large enough (hereafter, will be used interchangeably with the term macroscopic), these cross-correlations are negligible and can be completely ignored. Therefore the known thermodynamic relations in chemical equilibrium, observed to hold for macroscopic systems, are only private cases of a general formalism that permits fluctuations in the system.

Following the discovery of law of mass action[58], Langmuir invoked kinetics arguments to derive Eq. 2 and expressed the rate at which the A molecules adsorb onto the surface (the forward reaction in Eq. 1) as $k_{\text{ads}}\langle c_A\rangle_{eq}\langle\theta_S\rangle_{eq}$, where θ_S is the fraction of unoccupied sites. We further emphasize the values of c_A and θ_S correspond to values at equilibrium, each, averaged independently either over the duration of the measurements or over ensemble of configurations. This is because only when these quantities are considered uncorrelated, can the derivation proceed to yield Eq. 2. Applying our above mentioned argument of the necessity to include cross correlations also here, that is for expressing the bimolecular reaction rate, we claim in this paper that for small systems, Eq. 2 is not valid and another relation holds. Rephrased differently, consider two systems representing the adsorption process of Eq. 1 as sketched in Fig. 1. On the left, a single large system in the canonical

$(N_A^{\text{total}}, N_S^{\text{total}}, V, T)$ $m \times (n_A^{\text{total}}, n_S^{\text{total}}, v, T)$
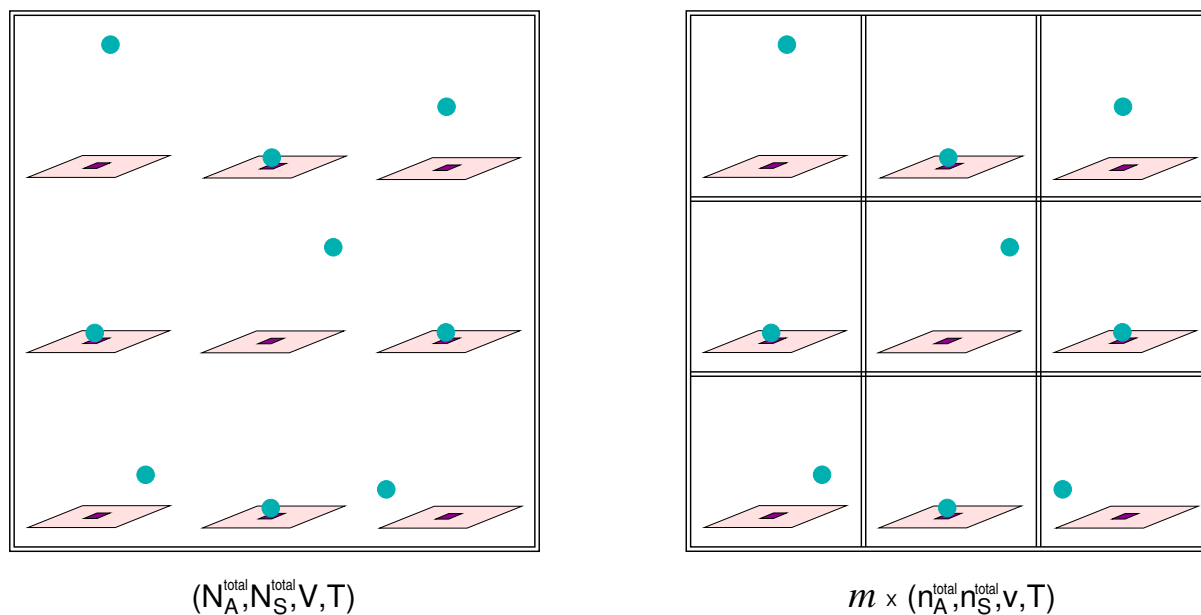
Figure 1: Left: a single large-sized system describing adsorption (Eq. 1) in the canonical ensemble $(N_A^{\text{total}}, N_S^{\text{total}}, V, T)$. Right: m isolated and independent small systems representing the same process where each system is in the canonical ensemble $(n_A^{\text{total}}, n_S^{\text{total}}, v, T)$. The gas molecules A are depicted by green balls, and the adsorbing sites S by purple squares. The fixed parameters of the systems on the left and right are related by, $N_A^{\text{total}} = m \cdot n_A^{\text{total}}$, $N_S^{\text{total}} = m \cdot n_S^{\text{total}}$, and $V = m \cdot v$.

ensemble $(N_A^{\text{total}}, N_S^{\text{total}}, V, T)$ is depicted, whereas on the right, m isolated and independent small

systems are shown, each of which is described by its own canonical ensemble $\left(n_A^{\text{total}}, n_S^{\text{total}}, v, T\right)$. It is argued here, that even if $N_A^{\text{total}} = m \cdot n_A^{\text{total}}$, $N_S^{\text{total}} = m \cdot n_S^{\text{total}}$, and $V = m \cdot v$, averages obtained in the large system on the left *are not equal* to those obtained by the m small systems on the right. Nonetheless, it is possible to transform averages observed at small systems to their corresponding values at macroscopic systems and vice versa. This can be performed by utilizing the equilibrium constant that, when accounts for cross-correlations in concentrations, has the same value independent of system's size, a property enabling it to link the chemical compositions of the two systems at equilibrium. We start by deriving a general expression of the equilibrium constant for adsorption.

Results

I. Derivation of the Equilibrium Constant for Adsorption

We consider the adsorption process specified in Eq. 1 as associations between gas particles A and immobile (surface) particles S to produce immobile bound products SA. It is assumed all components behave ideally, that means, except of the adsorption reaction described in Eq. 1, the particles do not interact with one another and a single adsorbing site can only interact with a single gas particle. Put another way, adsorption on a given site does not affect adsorptions on nearby sites and no multilayer adsorption is possible.

To obtain the expression of the equilibrium constant, K, at temperature T we utilize the definition,

$$K \equiv e^{-\Delta G^{\varnothing}/RT} \qquad , \tag{3}$$

where R is the gas constant and $\Delta G^{\varnothing}$, the standard Gibbs energy change of adsorption, is the change in Gibbs free energy when one mole of A adsorb onto one mole of S vacant sites to produce one mole of occupied sites, under conditions in which both the reactants and product are at their standard (reference) states. For a gas component the standard state is normally defined by a chosen value of its partial pressure, $P^{\varnothing}$, nevertheless, we find it convenient to specify instead the

corresponding standard concentration, $c^\varnothing$. If $N^\varnothing$ is the number of A particles which adsorb onto S sites when the reference reaction goes into completion (which at this point is not restricted to be one mole but only a large number), then the volume of the gas is $V^\varnothing = N^\varnothing/c^\varnothing$. The standard states of the immobile, vacant and occupied, sites are not consistently defined in the literature. This introduces no problem as long as these two standard states are the same. To advance with the derivation we choose their standard state to correspond to the particle number $N^\varnothing$. This can be expressed, for example, by surface density or concentration of the vacant/occupied sites, $N^\varnothing/A_S$, where A_S is the surface area of the adsorbent.

Applying a statistical mechanics framework, the reference system is chosen to be described by the canonical ensemble $(N_A^\varnothing, N_S^\varnothing, V^\varnothing, T)$ where $N_A^\varnothing = N_S^\varnothing = N^\varnothing$ are the number of A particles and S sites. We consider $V^\varnothing$ to correspond also to the volume of the whole system by assuming the excluded volumes of the A particles and S sites are negligible. The corresponding partition function can be expressed by,

$$Q^\varnothing = \frac{1}{N_A^\varnothing!} \sum_{i=0}^{N^\varnothing} \frac{N_A^\varnothing!}{(N_A^\varnothing - i)! \, i!} \, \frac{N_S^\varnothing!}{(N_S^\varnothing - i)!} \, (q_A^\varnothing)^{N^\varnothing - i} \, (q_S^\varnothing)^{N^\varnothing - i} \, (q_{SA}^\varnothing)^i \qquad , \qquad (4)$$

where summation over index i ($i \equiv N_{SA}$) includes all possible numbers of occupied SA sites, and thereby, all possible (interparticle) energy states. $q_A^\varnothing$ and $q_S^\varnothing$ are single-particle partition functions of an A particle in the gas phase and of a vacant S site, both, in the reference system. $q_{SA}^\varnothing$ is the pair-particle partition function of an occupied SA site (also in the reference system) which incorporates the Boltzmann factor of the adsorption energy. The division, outside the sum, by $N_A^\varnothing!$ is because the A gas particles are indistinguishable. In contrast, the immobile adsorbing sites S are distinguishable and therefore a corresponding division by $N_S^\varnothing!$ is not performed. The first and second fractions of factorials inside the sum express the degeneracy of state i. The first term counts the number of ways to choose i A particles out of $N_A^\varnothing$ particles where the order in the chosen group is not important. The second term represents the number of ways to distribute these i A particles into $N_S^\varnothing$ sites. Even though in the reference system $N_A^\varnothing = N_S^\varnothing = N^\varnothing$, we kept indicating the subscripts of the particle numbers in the terms of the factorials in Eq. 4 to clarify

their origin. Otherwise we obtain,

$$Q^\varnothing = N^\varnothing! \sum_{i=0}^{N^\varnothing} \frac{(q_A^\varnothing)^{N^\varnothing-i}}{(N^\varnothing-i)!} \frac{(q_S^\varnothing)^{N^\varnothing-i}}{(N^\varnothing-i)!} \frac{(q_{SA}^\varnothing)^i}{i!} \qquad . \tag{5}$$

Equation 5 is arranged in such a way that each (single- or pair-) particle partition function, raised to the power of its particle number, is divided by the factorial of this power. Yet it is worth emphasizing this division does not imply the S or SA sites are indistinguishable, but instead, it is a consequence of their equivalence (degeneracy in the energy of the state). In fact, the distinguishability of the S sites (either vacant or occupied) is manifested by the existence of the factor $N^\varnothing!$ outside the sum, which is absent for binding reactions where both reactants are indistinguishable[54].

We continue by expressing the Gibbs free energy change, $\Delta G_{0 \to N^\varnothing}$, when $N^\varnothing$ particles of A adsorb onto $N^\varnothing$ sites S. Then, $\Delta G^\varnothing$ is obtained by scaling $\Delta G_{0 \to N^\varnothing}$ to one mole. In a canonical ensemble, the partition function of the system is related to Helmholtz free energy. Therefore, the corresponding change in Helmholtz free energy, $\Delta F_{0 \to N_A^\varnothing}$, can be calculated from the ratio of the probability to find the system in the fully adsorbed state, p^{SA} (i.e., the fraction of the state $i = N^\varnothing$ in the sum of the partition function in Eq. 5), to the probability of the fully unadsorbed (or vacant) state, p^{A+S} (the fraction of the state $i = 0$). Note that the reference system is implied to be macroscopic as it reports a change in Gibbs energy per mole of stoichiometric reaction. This is the reason we restricted $N^\varnothing$ to be large. Thus, we can use the thermodynamic relation between Gibbs and Helmholtz free energies and write $\Delta G_{0 \to N^\varnothing}$ as,

$$\Delta G_{0 \to N^\varnothing} \equiv G_{i=N^\varnothing} - G_{i=0} = \Delta F_{0 \to N^\varnothing} + V^\varnothing \Delta P_{0 \to N^\varnothing} = -k_B T \ln \frac{p^{SA}}{p^{A+S}} + V^\varnothing \Delta P_{0 \to N^\varnothing}$$

$$= -k_B T \ln \left[\frac{(q_{SA}^\varnothing)^{N^\varnothing} N^\varnothing!}{(q_A^\varnothing)^{N^\varnothing} (q_S^\varnothing)^{N^\varnothing}} \right] + V^\varnothing \Delta P_{0 \to N^\varnothing} \qquad , \tag{6}$$

where $\Delta P_{0 \to N^\varnothing}$ is the change in pressure of the system when $N^\varnothing$ A gas particles are adsorbed. Noting $V^\varnothing \Delta P_{0 \to N^\varnothing}$ equals $-N^\varnothing k_B T$ for ideal gases and applying Stirling's approximation to evaluate $\ln N^\varnothing!$ we get,

$$\Delta G_{0 \to N^\varnothing} = -N^\varnothing k_B T \ln \frac{q_{SA}^\varnothing}{q_A^\varnothing / V^\varnothing \cdot q_S^\varnothing} - N^\varnothing k_B T \ln c^\varnothing \qquad , \tag{7}$$

8

an expression that is the same as that obtained for binding reactions when both reactants are mobile indistinguishable particles[54]. This is because the term in Eq. 5 characterizing the distinguishability of the immobile S sites cancels-out when calculating the ratio of probabilities in Eq. 6. Hence, from here the derivation of the expression of K is similar to that for a binding reaction, nonetheless, we will briefly outline the critical steps.

In the reference system we looked only at two states, $i = 0$ and $i = N^\varnothing$, from which $\Delta G^\varnothing$ is to be calculated. This reference reaction is hypothetical in the sense that full conversion is, in general, not attainable spontaneously. It turns out, we can evaluate $\Delta G^\varnothing$ of this reference system from equilibrium properties, spontaneously attainable, of a similar (generic) system at the same temperature but with arbitrary concentrations and size, which can be macroscopic or finite. The canonical ensemble of the generic system is specified by the parameters $(N_A^{\text{total}}, N_S^{\text{total}}, V, T)$, where $N_A^{\text{total}} = N_A + N_{SA}$ and $N_S^{\text{total}} = N_S + N_{SA}$ are total numbers of A particles and S sites, which are in general not equal. Its partition function is similar to Eq. 4 and takes the form,

$$Q = \frac{1}{N_A^{\text{total}}!} \sum_{i=0}^{N_{SA}^{\text{max}}} \frac{N_A^{\text{total}}!}{(N_A^{\text{total}} - i)! \; i!} \; \frac{N_S^{\text{total}}!}{(N_S^{\text{total}} - i)!} \; q_A^{N_A^{\text{total}} - i} \; q_S^{N_S^{\text{total}} - i} \; q_{SA}^{i} \quad , \tag{8}$$

where N_{SA}^{max} is the maximum number of occupied sites the system can support (i.e., $N_{SA}^{\text{max}} = N_A^{\text{total}}$ for $N_A^{\text{total}} \leq N_S^{\text{total}}$, or $N_{SA}^{\text{max}} = N_S^{\text{total}}$ otherwise).

To calculate $\Delta G^\varnothing$ by Eq. 7 requires the evaluation of the ratio $q_{SA}^\varnothing V^\varnothing / (q_A^\varnothing q_S^\varnothing)$. Being fixed in space, it is clear $q_S^\varnothing$ and $q_{SA}^\varnothing$ are equal to the corresponding particle partition functions of the generic system, q_S and q_{SA}. In contrast, due to translation, the single-particle partition function of A gas particle depends on the volume of the gas. If we approximate the discrete sum of quantum translational energy states by an integral[55], the dependency on volume can be shown to be linear and the following equality exist,

$$\frac{q_{SA}^\varnothing}{q_A^\varnothing / V^\varnothing \cdot q_S^\varnothing} = \frac{q_{SA}}{q_A / V \cdot q_S} \quad . \tag{9}$$

The validity of approximating the discrete sum with an integral is decreased with decreasing temperature, mass, and volume. However, it is shown to be well justified for almost all molecular systems

at relevant conditions[55]. We proceed by multiplying and dividing the ratio on the right-hand side of Eq. 9 by the term,

$$\sum_{i=0}^{N_{SA}^{\text{max}}-1} \frac{(i+1)}{\left[N_A^{\text{total}} - (i+1)\right]! \left[N_S^{\text{total}} - (i+1)\right]!(i+1)!} \; q_A^{N_A^{\text{total}}-i} \; q_S^{N_S^{\text{total}}-i} \; q_{SA}^{i} \qquad , \qquad (10)$$

and obtain,

$$\frac{q_{SA}}{q_A/V \cdot q_S} = V \frac{\sum_{i=0}^{N_{SA}^{\text{max}}-1} \frac{(i+1)}{\left[N_A^{\text{total}}-(i+1)\right]!\left[N_S^{\text{total}}-(i+1)\right]!(i+1)!} \; q_A^{N_A^{\text{total}}-(i+1)} \; q_S^{N_S^{\text{total}}-(i+1)} \; q_{SA}^{i+1}}{\sum_{i=0}^{N_{SA}^{\text{max}}-1} \frac{(i+1)}{\left[N_A^{\text{total}}-(i+1)\right]!\left[N_S^{\text{total}}-(i+1)\right]!(i+1)!} \; q_A^{N_A^{\text{total}}-i} \; q_S^{N_S^{\text{total}}-i} \; q_{SA}^{i}} \qquad . \qquad (11)$$

By applying a sequence of algebraic operations on the right-hand side of Eq. 11 (without introducing any further assumptions), it can be shown that[54],

$$\frac{q_{SA}^{\varnothing}}{q_A^{\varnothing}/V^{\varnothing} \cdot q_S^{\varnothing}} = \frac{q_{SA}}{q_A/V \cdot q_S} = V \frac{\langle N_{SA} \rangle}{\langle N_A N_S \rangle} \qquad , \qquad (12)$$

the ratio of particle partition functions reduces to a ratio of average number of occupied sites to average of product between number of unadsorbed A gas and number of vacant S sites, where both averages are taken at equilibrium conditions of the generic system. Inserting the equality in Eq. 12 into Eq. 7 and scaling $\Delta G_{0 \to N^{\varnothing}}$ to one mole yield,

$$\Delta G^{\varnothing} = -N_{\text{Avogadro}} k_B T \ln \frac{\langle N_{SA} \rangle V}{\langle N_A N_S \rangle} - N_{\text{Avogadro}} k_B T \ln c^{\varnothing} \qquad , \qquad (13)$$

from which K is obtained using its definition in Eq. 3,

$$K = \frac{\langle N_{SA} \rangle V c^{\varnothing}}{\langle N_A N_S \rangle} = \frac{\langle N_{SA} \rangle}{\langle (c_A/c^{\varnothing}) N_S \rangle} = \frac{\langle \theta_{SA} \rangle}{\langle (c_A/c^{\varnothing})(1 - \theta_{SA}) \rangle} \qquad , \qquad (14)$$

where $\theta_{SA} = N_{SA}/N_S^{\text{total}}$ is the fraction of occupied sites. The expression of K in Eq. 14 is different than that derived in textbooks and routinely utilized in the literature. The difference is that the latter ignores correlations between the reactants' particle-numbers/concentrations and is written as[59,60],

$$K' = \frac{\langle \theta_{SA} \rangle}{\langle (c_A/c^{\varnothing}) \rangle \langle (1 - \theta_{SA}) \rangle} \qquad . \qquad (15)$$

This neglect of cross-correlations is significant for small systems and renders the equilibrium constant K not constant for systems at the same temperature but with different concentrations or

sizes. The discrepancy of K' from K can reach few orders of magnitudes and is augmented for lower temperatures or stronger binding/adsorption energy, as well as, for higher concentrations. With increasing system size, K' approaches K, and for macroscopic systems these correlations in reactant's concentrations can be ignored.

II. Validations against Monte Carlo Simulations

We now test the predictions derived above against results obtained by Monte Carlo (MC) simulations. In short, we performed four series of simulations. In the first, R1, we increased $N_S^{\text{total}} = N_A^{\text{total}}$ from 1 to 120 and simultaneously increased the volume in such a way the concentration $c_A^{\text{total}} = N_A^{\text{total}}/V$ is constant at $\sim 0.013\ M$. The series R2 and R3 involved variations in particle-number of only one of the reacting species (either A gas or S adsorbing site) whereas the number of the other reactant was fixed. In these cases the volume also changed, subject to maintaining the concentration of the most abundant species constant ($\sim 0.025\ M$). More information about the systems, model particles, and computations is given in the Methods section.

In Fig. 2 we display the equilibrium constant for R1–R3 series of simulations. As should be the case, the value of K computed by Eq. 14 is constant for all systems of the three series. Due to different scales of the y-axis, it might be difficult to notice the average of K for all points in R1, 214.0 ± 0.3, is very similar to those for R2 and R3, 214.3 ± 0.3 and 214.2 ± 0.4, respectively. In contrast, the value of K' (Eq. 15) is not constant and varies significantly with system's size and concentration of N_S^{total} or N_A^{total}. Only at large system sizes, does the value of K' approach that of K and apparently it happens 'faster' in R1 series, compared to R2 and R3, likely because the concentration is lower. Note the maxima observed in R2 and R3, at $N_A^{\text{total}} = 4$ and $N_S^{\text{total}} = 4$, are because for smaller particle-numbers the most abundant species is that whose particle-number is fixed, whereas, for larger particle-numbers it is that with varying particle-number. To compare the equilibrium constant of adsorption, where one reactant is mobile and the other immobile, to that of binding, where both reactants are mobile, we repeated three points in R1 series, $N_S^{\text{total}} = N_A^{\text{total}} = 1, 8, 120$, but allowed the S particles to freely move in the simulation
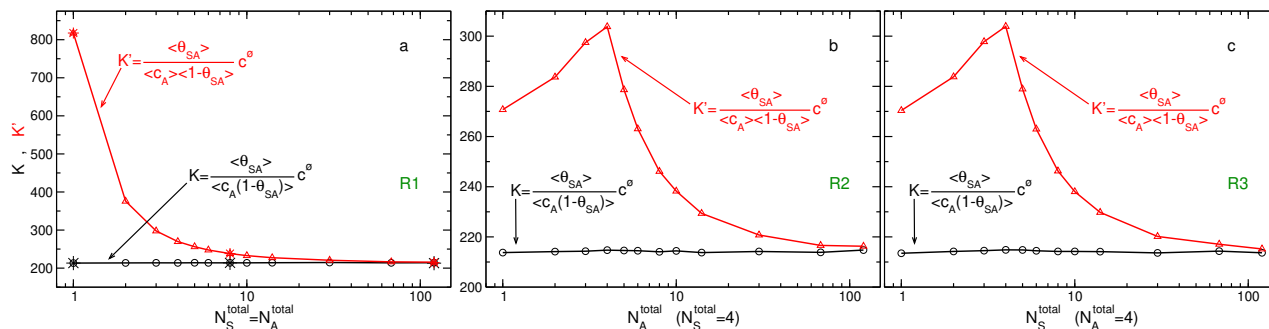
Figure 2: Equilibrium constant of adsorption K, defined in Eq. 14, for (a) R1 series of simulations as a function of total number of immobile (S) and mobile (A) particles, $N_S^{\text{total}} = N_A^{\text{total}}$, (b) R2 series as a function of N_A^{total} where N_S^{total} is fixed, and (c) R3 series as a function of N_S^{total} where N_A^{total} is fixed. For comparison, the conventional expression of the equilibrium constant ignoring two-body correlations K', defined in Eq. 15, is also displayed. The curves of K' in (b) and (c) seem identical, nonetheless they are distinct and were obtained independently. The star symbols in (a) at $N_S^{\text{total}} = N_A^{\text{total}} = 1, 8, 120$ correspond to additional simulations in which the S (along with the A) particles are mobile.

box. The results, displayed in Fig. 2 by star symbols, indicate the values of K (as well as K') are almost identical to those obtained by simulations of the adsorption process. Again, this is because K is described by ratio of probabilities of observing two-states, and the reduced phase-space (or distinguishability) in the system cancels-out when taking this ratio.

Given two variables of a system, ζ and η, it is well known from statistical mechanics that the average amplitude of their cross fluctuations relative to their mean values, $l(\zeta, \eta) = \langle (\zeta - \langle \zeta \rangle)(\eta - \langle \eta \rangle) \rangle / (\langle \zeta \rangle \langle \eta \rangle)$, decreases linearly with system's size[61]. Furthermore, these average fluctuations can be related to some properties, such as heat capacity, of the system[62,63]. In relation to bimolecular association reactions, it was shown that the average number of bound product is inversely proportional to two relative fluctuations in the system[54], which can be projected on the adsorption reaction described in Eq. 1 to yield,

$$\langle N_{SA} \rangle = \frac{1}{l(N_{SA}, N_{SA}) - l(N_{SA}, N_S N_A)} \qquad . \tag{16}$$

12

In Fig. 3 we examine this relation on R1–R3 series of simulations. The results, with points spanning
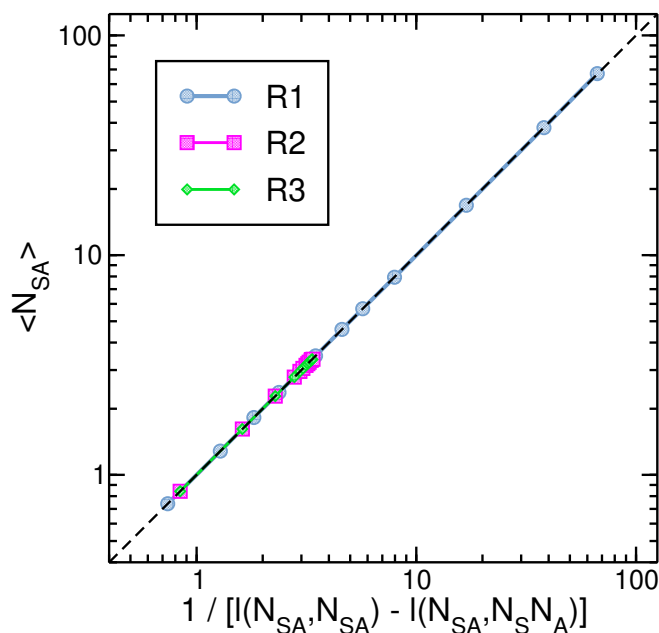

Figure 3: The relation between average number of adsorbed particles and the reciprocal of a difference between two relative fluctuations (Eq. 16). The dashed black line corresponds to $y = x$ and is shown as a reference for perfect agreement. The points of R2 series almost overlap those of R3.

approximately two-orders of magnitude in values, indicate an excellent agreement with theory.

III. Prediction of Surface Coverage from the Equilibrium Constant

Even though the equality in Eq. 16 provides a route to predict average number of occupied sites from fluctuations in the system, there are benefits to establish an alternative relation in which the required quantities do not need to be extracted from the system in question. In effect, this is the reason why equilibrium constant is so important; its value and the parameters specifying a desired system (e.g., $N_A^{\text{total}}, N_S^{\text{total}}, V, T$) can predict the chemical composition of that system. This is well known for macroscopic systems where the solution for θ_{SA} in Eq. 15 is straightforward and yield the Langmuir adsorption isotherm equation[1] shown in Eq. 2. In Fig. 4 we display the average fraction of occupied sites, $\langle \theta_{SA} \rangle$, observed in the simulations for R1–R3 series. Predictions based
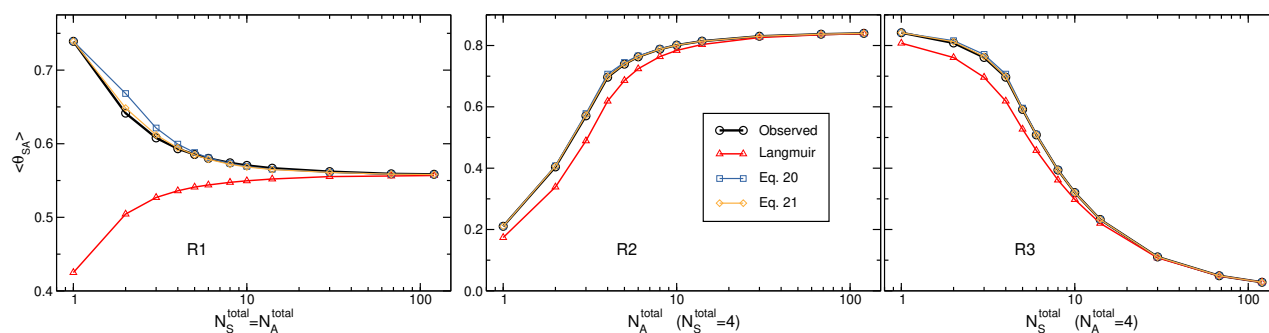
Figure 4: Predictions of average number of occupied adsorbing sites, presented here as average fraction $\langle \theta_{SA} \rangle = \langle N_{SA} \rangle / N_S^{\text{total}}$, from the value of K and parameters specifying the system. Results based on Langmuir Adsorption Isotherm (red, triangles) are calculated by Eq. 2 where the value of K is that determined for a macroscopic system. Also displayed are results based on Eq. 17 using an approximation to evaluate $l(N_{SA}, N_{SA})$ (Eq. 19). In a previously proposed empirical relation[54], the value of λ appearing in Eq. 19 is given by Eq. 20 (blue, squares), whereas in current work it is proposed to be given by Eq. 21 (orange, diamonds). Values of $\langle \theta_{SA} \rangle$ observed directly in the simulations are shown as references (black, circles).

on Langmuir adsorption isotherm indicate that for R2 and R3 series, the predicting curves deviate moderately from the curve determined by direct counting from the simulation of each system. In fact the shapes of the curves are similar and at large numbers of particles (either N_A^{total} in R2 or N_S^{total} in R3) the predictions are excellent. Very good predictions are also exhibited in R1 series at the two largest numbers of particles, however for smaller numbers, significant discrepancies are observed with magnitudes intensifying as $N_S^{\text{total}} = N_A^{\text{total}}$ decreases. For example, the observed value of $\langle \theta_{SA} \rangle$ in the simulation at $N_S^{\text{total}} = N_A^{\text{total}} = 1$ is 0.74 whereas Langmuir equation predicts a value of 0.42.

In principle, one can solve for $\langle \theta_{SA} \rangle$ in Eq. 14, however, because of cross correlations in particles numbers of A and S this is not so simple. Yet, it is easy to show that,

$$\langle \theta_{SA} \rangle = \frac{\left(N_A^{\text{total}} + N_S^{\text{total}} + \frac{Vc^{\varnothing}}{K}\right) - \sqrt{\left(N_A^{\text{total}} + N_S^{\text{total}} + \frac{Vc^{\varnothing}}{K}\right)^2 - 4N_A^{\text{total}} N_S^{\text{total}} \left[l(N_{SA}, N_{SA}) + 1\right]}}{2\left[l(N_{SA}, N_{SA}) + 1\right] N_S^{\text{total}}} ,$$

(17)

14

where $l(N_{SA}, N_{SA})$ are relative fluctuations in the number of occupied sites. That means, the average number $\langle N_{SA} \rangle$ can be calculated from its spread. For macroscopic systems, $N_S^{\text{total}}, N_A^{\text{total}} \to \infty$, we know $l(N_{SA}, N_{SA}) \to 0$, and $\langle \theta_{SA} \rangle$ can be easily obtained from Eq. 17. The other extreme case, which is also solvable, is when the total number of, at least, one component equals one. In these systems $\langle N_{SA}^2 \rangle = \langle N_{SA} \rangle$, and therefore the relative fluctuations are related to K by the (exact) relation,

$$l(N_{SA}, N_{SA})_{N_Y^{\text{total}}=1} = \frac{V c^{\varnothing}}{K N_X^{\text{total}}} \qquad , \tag{18}$$

where X refers to the more abundant component, $N_X^{\text{total}} \geq N_Y^{\text{total}}$, regardless being the gas particles or the immobile adsorbing sites.

Based on the behavior of $l(N_{SA}, N_{SA})$ described in Eq. 18 and in the thermodynamic limit, in a previous publication we suggested an empirical interpolation applicable for all possible particle numbers[54],

$$l(N_{SA}, N_{SA}) \simeq \frac{V c^{\varnothing}}{K N_X^{\text{total}} (N_Y^{\text{total}})^{\lambda}} \qquad , \tag{19}$$

where λ equals,

$$\lambda = \frac{1}{1 + K/\left(V c^{\varnothing} \ln N_X^{\text{total}}\right)} \qquad . \tag{20}$$

Thus Eq. 20 and Eq. 19 can be used together with Eq. 17 to yield an approximation for the average fraction of occupied sites from only the value of K (and the parameters specifying the system). The results, shown in Fig. 4, exhibit very good agreement with values observed directly in the simulations, and for finite systems significantly improves the predictions calculated by the Langmuir equation. Nevertheless for some points, $N_S^{\text{total}} = N_A^{\text{total}} = 2, 3, 4$ in R1 series, the predictions are noticeably imperfect. That being so, we re-evaluated empirically the suggested value of λ and found an alternative expression that predicts better the observed results,

$$\lambda = \frac{1}{1 + K/\left(V c^{\varnothing} \sqrt{N_X^{\text{total}}}\right)} \qquad . \tag{21}$$

The results of this new approximation are shown in Fig. 4 as well, demonstrating excellent agreement relative to direct counting with almost unnoticeable discrepancies. In order to test whether

the new approximation to evaluate $l(N_{SA}, N_{SA})$ given in Eq. 21 would also improve the predictions made in a previous work, we applied it for binding reactions for all systems investigated previously. The results are presented in Fig. SI-1 and Fig. SI-2 of the Supporting Information. In all 52 systems examined, agreement with direct counting is excellent, and in all points where previous approximation (Eq. 20) displayed noticeable discrepancies, predictions based on current approximation (Eq. 21) offer significant and satisfactory improvements.

The systems in R1–R3 series were all performed with the same strength of adsorption energy, which means when combined with conditions of constant temperature, the resulting equilibrium constant is the same for all systems. Therefore, in order to test the performance of the proposed predictions for a range of values of K, we performed a fourth series of simulations, R4, wherein the well-depth of the LJ potential between the gas particles and the adsorbing sites are modified systematically from $15.0 \ kJ/mol$ to $50.0 \ kJ/mol$ in equal steps of $5.0 \ kJ/mol$. We chose the finite system of $N_S^{\text{total}} = N_A^{\text{total}} = 2$ because it displayed the largest discrepancies with our predictions (pointing out once again, the private case in which the particle number of, at least, one of the components equals one, can be solved exactly). As shown in Fig. 5a, the variations in the strength of the adsorption energy produces equilibrium constants that range from $2 \cdot 10^{-1}$, for the weakest interaction, to $7 \cdot 10^4$, for the strongest interaction. Substantial deviations of K' from K start at around $\epsilon_{SA} = 30 \ kJ/mol$ and rapidly intensify with an increase in the adsorption energy. For example the relative deviation, $(K' - K)/K$, is $1.4 \cdot 10^{-3}$ for $\epsilon_{SA} = 15 \ kJ/mol$, whereas, it is 230 for $\epsilon_{SA} = 50 \ kJ/mol$. In Fig. 5b the relation between average number of occupied sites and the reciprocal of a difference between two relative fluctuations in the system, as described in Eq. 16, is plotted. The results indicate an almost perfect agreement. Moreover, the predictions of computing $\langle \theta_{SA} \rangle$ from K are examined in Fig. 5c. Langmuir adsorption isotherm model predicts the occupancy very well at weak adsorption energies (or high temperatures) but fails when the adsorption is strong (low temperatures). In fact the discrepancies of the predictions reflects the deviations of K' from K. Predicting $\langle \theta_{SA} \rangle$ by approximating $l(N_{SA}, N_{SA})$ (Eq. 18) using λ given by Eq. 20 is very good even at strong adsorption energies. Nonetheless when λ is given by Eq. 21,
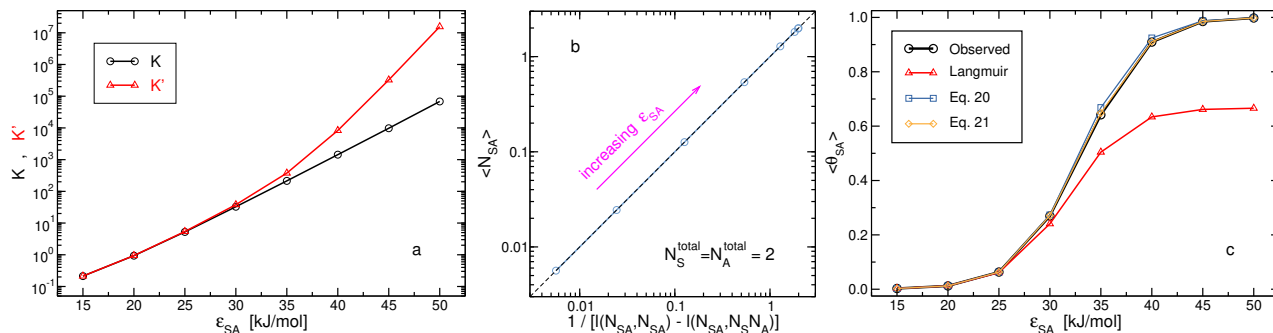
Figure 5: Results from R4 series of simulations in which the adsorption energy ($\epsilon_{SA} = 35 \ kJ/mol$ in R1–R3) is systematically modified in the range $15-50 \ kJ/mol$. In all R4 systems, $N_S^{\text{total}} = N_A^{\text{total}} = 2$ and $c_A^{\text{total}} = 0.008 \ molecules/nm^3$. (a) The equilibrium constant, K (Eq. 14), and the conventional expression ignoring correlations, K' (Eq. 15), as a function of ϵ_{SA}. (b) The relation between average number of occupied sites and relative fluctuations (Eq. 16). Note that at $\langle N_{SA} \rangle \simeq 2$, there are two points that are almost completely overlapping. (c) Predictions of average fraction of occupied sites as a function of ϵ_{SA}. Colors and symbols of the different curves are the same as those in Fig. 4.

the predictions are further improved and almost coincide with direct counting.

Taken together, the results presented in Fig. 2, 4, and 5 point also to the complexity of assigning a priori a minimum size to a system, above which it behaves macroscopically. The reason is that this minimum size depends on five parameters. Two of these parameters, temperature and adsorption energy, can be represented by a single parameter, the reduced temperature $k_B T / \epsilon_{SA}$. The thermodynamic limit is hence approached by increasing this reduced temperature, number of particles N_S^{total} and N_A^{total}, and volume V (see Fig. 1b in a previous work[54]). The extent to which the term $K'/K - 1$ approaches zero can then serve as a descriptor for macroscopic behavior, and a choice of a threshold value, classifies the system as macroscopic or finite. By definition, the term $K'/K - 1$ equals $l(N_A, N_S)$. However, our attempts to relate these relative fluctuations to the four parameters mentioned above met with no success.

On a last note, the curve of $\ln K$ as a function of ϵ_{SA} shown in Fig. 5a is almost linear

(linear regression yields correlation coefficient of 0.9993). This is because the two-body particle partition function of an occupied site, q_{S_A}, contains the factor $e^{-U_{SA}/RT}$, where U_{SA} is the effective adsorption energy, proportional to ϵ_{SA} but with a negative sign, and it implies the slope of the line equals $1/RT = 0.401\ mol/kJ$. However the linear-regression of the simulation data points yields a slope of $0.366\ mol/kJ$. We conjecture this difference, as well as the small deviation of the correlation coefficient from 1, arise due to changes in vibrational energy of an occupied site with changes of ϵ_{SA}.

Discussion

I. Chemical Equilibrium of Adsorption in a Grand Canonical Ensemble

Derivation of Langmuir adsorption isotherm, within a statistical mechanics framework, is customary performed in the literature by the grand-canonical ensemble[25]. In this ensemble, the chemical potential of the adsorbate, μ_A, is constant by coupling the system to a bulk reservoir of A, whereas, its particle number (or concentration) is subject to fluctuations. Yet, the familiar relation for ideal systems between chemical potential, relative to that at standard state, and concentration,

$$\mu_A = \mu_A^\varnothing + RT \ln \frac{c_A}{c^\varnothing} \qquad , \tag{22}$$

implies that fixing the chemical potential necessarily fixes the concentration. This situation holds for macroscopic systems, because if N_A is large and the system is completely open to a bulk reservoir of A, the variations in concentration (due to adsorptions and desorptions at equilibrium) are very small and can be rapidly compensated by diffusion of A between reservoir and system. Then, the emerging properties of the system are properly defined by a grand canonical ensemble and cross-correlations in particle numbers are decoupled, yielding Langmuir's equation (Eq. 2).

Consider now a small open system, that is, a small adsorbing surface (i.e., small N_S) in contact with a small volume containing A which is open to a reservoir of A. If the migration relaxation time of A, to and from, the reservoir is faster than the adsorption/desorption times, then, to a very good approximation, the chemical potential and concentration of A in the small system are constant, and consequently, Langmuir's equation is obeyed as well.

However, if the diffusion relaxation time of A between the small system and reservoir is slower than adsorption/desorption times, an ensemble with mixed properties emerges. This can happen if the concentration of A is very low, or if the system is defined as small by a physical confinement and at the same time is coupled to a reservoir of A. In the latter, the boundaries of the small system do not permit mass exchange, except of a small region, for example, with a size on the order of that of A. In this scenario, constant chemical potential and concentration of A are only partially observed. Albeit not conforming to any thermodynamic ensemble, one can argue that

such a system can be represented as a hybrid between canonical and grand-canonical ensembles. Although this may be possible to approximate by interpolation, we do not attempt to address this case here and limit our derivation only to the canonical ensemble which is closed to mass transfer.

II. Experimental Realizations of Closed Small Systems

Testing the predictions made in this paper requires the ability to monitor localizations of mass at the single molecule level. Technically, such capability was reported three and a half decades ago in crystals[64] and soon after in solutions[65]. An additional requirement is the capacity to confine the monitored molecules to a small system, normally characterized by a small volume. This can be realized by several methods. For example, surfactant-stabilized aqueous droplets can form confined 'containers' with pico- to atto-liter volume[66–71] wherein reactions involving small numbers of chemical components can be followed, usually with fluorescence microscopy[72,73]. Another example is imaging the behavior of biomolecules in living cells[74] and exosomes[75]. In this respect the use of synthetic vesicles such as liposomes, which are widely utilized as pharmaceutical nanocarriers[76], can provide better control on the identity and concentrations of the different encapsulated molecules[77–79]. To increase accuracy in reading fluorescence signals, the liposomes in bulk solution are often immobilized by surface tethering[80]. Of a particular interest to the proposed statistical analysis is the embedding of transmembrane proteins across the bilayer lipid membrane of the vesicle[81–84]. In these systems the proteins' cytosolic receptors can bind with encapsulated ligands at varying concentrations. Being immobile within the lipid bilayer structure, these receptors can be identified as surface sites and the ligands as adsorbate molecules in the adsorption model addressed in this paper.

III. An Application to an Experimental System

We now elaborate on a specific closed small system in which $N_A^{\text{total}} = N_S^{\text{total}} = 1$. Here, there are only two possible macroscopic states in the system, one corresponding to the adsorbed state, SA,

and the other, to the unadsorbed state, $A + S$. If the fluorescence emission signals indicate the fraction of time, thus the probability, of observing the adsorbed state is $p^{SA} = \langle N_{SA} \rangle$ (which means the fraction, or probability, of the unadsorbed state is $p^{A+S} = 1 - p^{SA} = \langle N_A N_S \rangle$), the expression of K in Eq. 14 becomes[39,54],

$$K_{N_A^{\text{total}} = N_S^{\text{total}} = 1} = \frac{p^{SA}}{p^{A+S}} \, V c^{\varnothing} = \frac{p^{SA}}{1 - p^{SA}} \, V c^{\varnothing} \qquad . \tag{23}$$

This system, in which one adsorbate molecule interact with one binding site has been constructed experimentally for tracking the kinetic and thermodynamic behavior of single molecules. One of the advantages of such a system is that fluorescence resonance energy transfer (FRET) measurements are facilitated[85]. More specifically, in order to increase reading accuracy in FRET experiments, the fluorescence signals ought to be spatially separated, limiting the studied systems to those containing low concentrations of interacting particles, which in turn restrict the investigations to adsorbate-adsorbent (or protein-receptor) pairs with large binding affinities. However, if these chemical species are encapsulated inside a vesicle with a small volume (e.g., a diameter of $100 \, nm$ yields approximately an atto-liter volume) their concentrations can be large, but at the same time, the optical signals can be spatially well resolved provided the distance between the surface tethered vesicles are large enough. For example, Chen and coworkers[86,87] studied the interactions between copper chaperone Hah1 protein and Wilson disease protein (WDP). The latter is a multidomain protein that is anchored to organelle membranes. The preparation of the nanovesicles was designed to encapsulate only one pair of proteins and the analyzes of the data were performed only from vesicles adhering to this content. To obtain the bimolecular dissociation constant between A and B proteins, the following expression, $K_D = (p^{A+B}/p^{AB})(1/V)$ was used. Apart from the standard concentration (introduced to render the equilibrium constant unitless), this expression is the reciprocal of the binding constant described in Eq. 23. Likewise, in calculating the bimolecular reaction rate constant[86,88,89], k, the observed reaction rate, $d(c_{AB})/dt$, is equated to the term $k\langle c_A \rangle (1/V)$. We emphasize that the expressions utilized for the dissociation constant and bimolecular rate constant *are not the same* as those known from chemistry textbooks. The authors of the

experimental studies argue that "for the single-molecule reaction occurring in a nanovesicle" the concentration of one of the particles (B) should be substituted by the term $1/V$ which represents an "effective concentration of one molecule inside the nanovesicle". Our interpretation is that this term follows from the requirement to take into account cross-correlations in concentrations, that is, $K_D = \langle c_A c_B \rangle / \langle c_{AB} \rangle$, and the rate of product formation equals $k \langle c_A c_B \rangle$. Then, for a system with $N_A^{\text{total}} = N_S^{\text{total}} = 1$, the two-body average, $\langle c_A c_B \rangle$, reduces to a one-body average, $\langle c_A \rangle (1/V)$. Note as well that for this private case, the probabilities are proportional to the corresponding concentrations, $p^{AB} = V \langle c_{AB} \rangle$ and $p^{A+B} = V \langle c_A \rangle = V \langle c_B \rangle = V^2 \langle c_A c_B \rangle$.

Conclusions

Due to their large amplitudes of fluctuations, properties of finite systems can be determined only by averaging over time or over configurations, and because adsorption is a two-body process, averaging its reaction rate necessitates the inclusion of cross correlations in reactant's concentrations. For this reason, Langmuir's equation breaks down when the number of adsorbate molecules and/or adsorbing sites are small. In this paper, we derived a general expression of the equilibrium constant for adsorption, K, that is valid also at small scales for closed systems. Despite the distinguishable character of the adsorbing sites, the expression obtained is the same as that for binding reactions where both reactants are indistinguishable particles. Moreover it is shown, this expression of K yields values that are constant upon changes in concentrations and system's size, down to the smallest system possible. In addition, we present an alternative equation to Langmuir adsorption isotherm where the expression of the fluctuations, $l(N_{SA}, N_{SA})$, is approximated by interpolation between two extreme cases that can be solved exactly; the thermodynamic limit and small systems where particle number of at least one reactant equals one. Given value of the equilibrium constant and total number of adsorbing sites, N_S^{total}, this proposed adsorption equation (Eqs. 17, 19 and 21) predicted almost perfectly the fraction of occupied sites observed by four series of simulations modeled by Monte Carlo technique. Note, in contrast to Langmuir's equation (Eq. 2), Eq. 17 requires knowledge also of the system's volume, V. Nonetheless when V, K, and N_S^{total} are not available, the amount of molecules adsorbed, $\langle N_{SA} \rangle$, can be plotted as a function of the total amount of adsorbate molecules introduced into the system, N_A^{total}. Then, the (non-linear) curve fitting can consider the term $V c^{\varnothing}/K$ as a single parameter which, together with N_S^{total}, reduces the number of fitted-parameters to two.

Computational Details

The model system consists of N_S^{total} adsorbing sites, S, each composed of two particles, s and h, whose Cartesian coordinates were fixed throughout the simulations. x and y coordinates of s and h particles were the same and correspond to a two-dimensional equilateral triangular lattice. z-components of all s particles equaled $2.50\ nm$, coinciding with the mid-point (along the z-axis) of the rectangular simulation box. The h particles were placed at $z = 2.64\ nm$, thus $0.14\ nm$ away from the s particles, and functioned as protecting groups to prevent binding of more than one adsorbate to a single adsorbing site. Nearest neighbor distances between S sites equaled $3.5\ nm$ and the shape of the triangular lattice formed by the N_S^{total} sites was chosen to generate, as much as possible, equal dimensions along the x- and y-axes (see Fig. 6).

N_A^{total} adsorbate molecules, A, in the gas phase are introduced randomly into the simulation box. Each A molecule is composed of two atoms, a and h, 'covalently' bonded with a bond-length of $0.14\ nm$. All atom-sites in the system have zero charge, $q_s = q_a = q_h = 0.0\ e$, and their intermolecular interactions are described by Lennard-Jones (LJ) potentials truncated at a distance of $2.0\ nm$. LJ parameters, σ and ϵ, for the interactions between different atom-sites are specified in Table 1. With these parameters, all interactions are effectively repulsive except for a strong

Table 1: Intermolecular Lennard-Jones parameters between immobile adsorbing sites, $S(sh)$, and adsorbate molecules, $A(ah)$, as well as, between the adsorbate molecules themselves.

	$\sigma\ [nm]$	$\epsilon\ [kJ/mol]$
$a \cdots a$	0.75	0.1
$h \cdots h$	0.50	0.1
$s \cdots h$	0.35	0.1
$a \cdots h$	0.35	0.1
$s \cdots a$	0.18	35.0

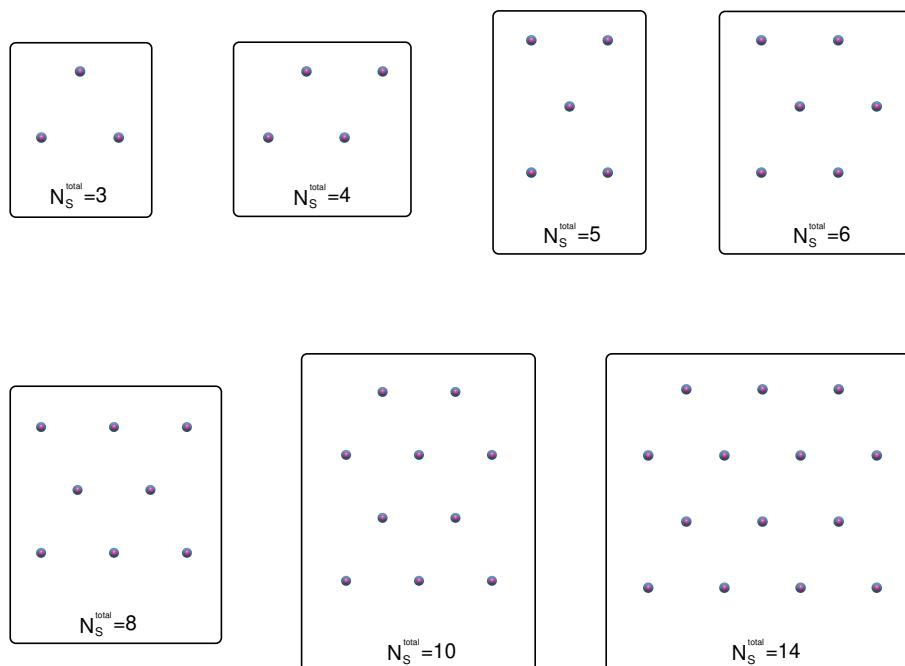attraction between the s and a atoms, resulting in adsorptions of one A molecule onto one S

Figure 6: Configurations of immobile adsorbing sites S for $3 \leq N_S^{\text{total}} \leq 14$ projected onto the xy-plane. s particles are depicted in magenta whereas h particles in blue. All sites have the same z-coordinates forming a two-dimensional equilateral triangular lattice with nearest neighbor distance of $3.5\ nm$. The configurations for $N_S^{\text{total}} = 1, 2$ are trivial, those for $N_S^{\text{total}} = 30\ (120)$ are built by $6\ (12)$ rows of $5\ (10)$ sites, whereas that for $N_S^{\text{total}} = 68$ is built by 5 rows of 8 alternating with 4 rows of 7 sites.

surface site, and this adsorption site (whether occupied or non-occupied) does not interact with any other surface sites. To define a state of an occupied (bound) site, a cutoff value of the interparticle distance between s and a is utilized, $r_{sa} < 0.37\ nm$, which captures the width of the first maximum (observed at $r_{sa} = 0.204\ nm$) in plots of all $g_{sa}(r)$'s. With this cutoff distance, the number of times in which two A molecules were counted as occupying the same S site were negligible. More explicitly, these 'doubly-occupied-sites' incidents were recorded only in R1 series for $N_S^{\text{total}} = N_A^{\text{total}} \geq 30$ with average numbers smaller than $3 \cdot 10^{-6}$.

All simulations were performed in the canonical $(N_A^{\text{total}}, N_S^{\text{total}}, V, T)$ ensemble with $T = 300\ K$. Total numbers of A particles and S sites, as well as volume, were varied systematically in dif-

ferent simulations. Changes in volumes are achieved by modifying the length of the rectangular simulation box along x- and y-axes, $L_{x,box} = L_{y,box}$, while maintaining $L_{z,box} = 5.00\ nm$ constant. Four series of simulations were constructed. In the first, R1, the value of $N_A^{\text{total}} = N_S^{\text{total}}$ equaled $1, 2, 3, 4, 5, 6, 8, 10, 14, 30, 68, 120$ keeping the concentration $c_A^{\text{total}} = N_A^{\text{total}}/V$ constant at $0.008\ molecules/nm^3$ ($\sim 0.013\ M$). Thus, values of $L_{x,box} = L_{y,box}$ ranged from $5.0\ nm$ for the smallest system to $54.77\ nm$ for the largest system. In the second series of simulations, R2, the number of surface sites was fixed, $N_S^{\text{total}} = 4$, whereas N_A^{total} varied from 1 to 120. On the other hand in the third series, R3, $N_A^{\text{total}} = 4$ is fixed while N_S^{total} ranged from 1 to 120. In both R2 and R3, the concentration of the most abundant species, c_S^{total} or c_A^{total}, is kept constant at $0.015\ molecules/nm^3$ ($\sim 0.025\ M$). We also performed simulations, R4 series, in which the adsorption energy is systematically varied. To this end, the LJ parameter ϵ between s and a atom sites (ϵ_{SA}) increased from $15.0\ kJ/mol$ to $50.0\ kJ/mol$ in locksteps of $5.0\ kJ/mol$, keeping all other parameters in the system the same as indicated in Table 1. We chose to conduct R4 series with $N_S^{\text{total}} = N_A^{\text{total}} = 2$ at $c_A^{\text{total}} = 0.008\ molecules/nm^3$ (thus, $L_{x,box} = L_{y,box} \simeq 7.07\ nm$) because this system exhibits the largest deviation with our previously proposed prediction of surface coverage.

Generations of different system's configurations forming a canonical ensemble were done by the Monte-Carlo (MC) method[90,91], coded in-house and ran in double-precision arithmetic. Periodic boundary conditions were applied along all three Cartesian axes. The Metropolis acceptance criterion[92] was applied to either accept or reject trial moves. Each trial move is composed of randomly selecting one A molecule which is then displaced, in each of the three Cartesian-axes, and rotated around each of the two axes perpendicular to the molecular axis. These displacements and rotations are performed as rigid bodies. Their magnitudes and directions were determined randomly from a uniform distribution with maximum values of $0.4\ nm$ for displacements along each of the Cartesian-axes, 0.1 for $\cos\theta$ when rotating around angle θ ($0 \leq \theta \leq \pi$), and $0.314\ rad$ for rotations around angle ϕ ($0 \leq \phi \leq 2\pi$). These trial moves resulted in acceptance-ratios that for R1–R3 series varied from 0.162 (R2, $N_A^{\text{total}} = 1$) to 0.964 (R2, $N_A^{\text{total}} = 120$), and for R4 series ranged from 0.006 ($\epsilon_{SA} = 50.0\ kJ/mol$) to 0.993 ($\epsilon_{SA} = 15.0\ kJ/mol$). For all systems, at least

5×10^9 trial moves were taken for equilibration. The number of trial moves for data collection was, approximately, inversely proportional to the size of the system. More specifically, in R1 series data collected by 1.0×10^{12} trial moves for the smallest system and by 1.2×10^{10} trial moves for the largest system. In R2 and R3 series, these numbers ranged from 5.0×10^{11} to 2.4×10^{10} trial moves, whereas in R4 series it equaled 1.2×10^{11} for all simulations.

Acknowledgments

References

[1] Langmuir, I. The Adsorption of Gases on Plane Surfaces of Glass, Mica and Platinum, *J. Am. Chem. Soc.* **1918**, *40*, 1361–1403.

[2] McMillan, W. G.; Mayer, J. E. The Statistical Thermodynamics of Multicomponent Systems, *J. Chem. Phys.* **1945**, *13*, 276–305.

[3] Burns, R. A.; El-Sayed, M. Y.; Roberts, M. F. Kinetic model for surface-active enzymes based on the Langmuir adsorption isotherm: phospholipase C (Bacillus cereus) activity toward dimyristoyl phosphatidylcholine/detergent micelles, *Proc. Natl. Acad. Sci. USA* **1982**, *79*, 4902–4906.

[4] Leng, X.; Starchev, K.; Buffle, J. Adsorption of Fluorescent Dyes on Oxide Nanoparticles Studied by Fluorescence Correlation Spectroscopy, *Langmuir* **2002**, *18*, 7602–7608.

[5] Sekine, T.; Nakatani, K. Intraparticle Diffusion and Adsorption Isotherm for Sorption in Silica Gel Studied by Single-Microparticle Injection and Microabsorption Methods, *Langmuir* **2002**, *18*, 694–697.

[6] Damian, A.; Omanovic, S. Interactive Adsorption Behavior of NAD^+ at a Gold Electrode Surface, *Langmuir* **2007**, *23*, 3162–3171.

[7] Cullen, S. P.; Liu, X.; Mandel, I. C.; Himpsel, F. J.; Gopalan, P. Polymeric Brushes as Functional Templates for Immobilizing Ribonuclease A: Study of Binding Kinetics and Activity, *Langmuir* **2008**, *24*, 913–920.

[8] Foo, K.; Hameed, B. Insights into the modeling of adsorption isotherm systems, *Chem. Eng. J.* **2010**, *156*, 2–10.

[9] Felsovalyi, F.; Mangiagalli, P.; Bureau, C.; Kumar, S. K.; Banta, S. Reversibility of the Adsorption of Lysozyme on Silica, *Langmuir* **2008**, *24*, 2569–2572.

[10] Louguet, S.; Kumar, A. C.; Guidolin, N.; Sigaud, G.; Duguet, E.; Lecommandoux, S.; Schatz, C. Control of the PEO Chain Conformation on Nanoparticles by Adsorption of PEO-block-Poly(L-lysine) Copolymers and Its Significance on Colloidal Stability and Protein Repellency, *Langmuir* **2011**, *27*, 12891–12901.

[11] Carr, R.; Comer, J.; Ginsberg, M. D.; Aksimentiev, A. Microscopic Perspective on the Adsorption Isotherm of a Heterogeneous Surface, *J. Phys. Chem. Lett.* **2011**, *2*, 1804–1807.

[12] Bharti, B.; Meissner, J.; Findenegg, G. H. Aggregation of Silica Nanoparticles Directed by Adsorption of Lysozyme, *Langmuir* **2011**, *27*, 9823–9833.

[13] Park, Y.; Ju, Y.; Park, D.; Lee, C.-H. Adsorption equilibria and kinetics of six pure gases on pelletized zeolite 13X up to 1.0MPa: CO_2, CO, N_2, CH_4, Ar and H_2, *Chem. Eng. J.* **2016**, *292*, 348–365.

[14] Meconi, G. M.; Ballard, N.; Asua, J. M.; Zangi, R. Adsorption and Desorption Behavior of Ionic and Nonionic Surfactants on Polymer Surfaces, *Soft Matter* **2016**, *12*, 9692–9704.

[15] Kundu, A.; Piccini, G.; Sillar, K.; Sauer, J. Ab Initio Prediction of Adsorption Isotherms for Small Molecules in Metal-Organic Frameworks, *J. Am. Chem. Soc.* **2016**, *138*, 14047–14056.

[16] Ayawei, N.; Ebelegi, A. N.; Wankasi, D. Modelling and Interpretation of Adsorption Isotherms, *J. Chem.* **2017**, *2017*, 3039817.

[17] Swenson, H.; Stadie, N. P. Langmuir's Theory of Adsorption: A Centennial Review, *Langmuir* **2019**, *35*, 5409–5426.

[18] Zhang, J.; Wang, J.; Zhang, C.; Li, Z.; Zhu, J.; Lu, B. Molecular simulation of gases competitive adsorption in lignite and analysis of original CO desorption, *J. Chem.* **2021**, *11*, 11706.

[19] Pelalak, R.; Soltani, R.; Heidari, Z.; Malekshah, R. E.; Aallaei, M.; Marjani, A.; Rezakazemi, M.; Shirazian, S. Synthesis, molecular dynamics simulation and adsorption study of different pollutants on functionalized mesosilica, *Langmuir* **2021**, *11*, 1967.

[20] Kalam, S.; Abu-Khamsin, S. A.; Kamal, M. S.; Patil, S. Surfactant Adsorption Isotherms: A Review, *ACS Omega* **2021**, *6*, 32342–32348.

[21] Sillar, K.; Kundu, A.; Sauer, J. Ab Initio Adsorption Isotherms for Molecules with Lateral Interactions: CO_2 in Metal-Organic Frameworks, *J. Phys. Chem. C* **2017**, *121*, 12789–12799.

[22] Kinniburgh, D. G. General Purpose Adsorption Isotherms, *Environ. Sci. Techno.* **1986**, *20*, 895–904.

[23] Boulinguiez, B.; Cloirec, P. L.; Wolbert, D. Revisiting the Determination of Langmuir Parameters-Application to Tetrahydrothiophene Adsorption onto Activated Carbon, *Langmuir* **2008**, *24*, 6420–6424.

[24] Chen, X. Modeling of Experimental Adsorption Isotherm Data, *Information* **2015**, *6*, 14–22.

[25] Volmer, M. Thermodynamische Folgerungen ans der Zustandsgleichung für adsorbierte Stoffe, *Z. Phys. Chem.* **1925**, *115U*, 253–260.

[26] Polak, M.; Rubinovich, L. Adsorption under nanoconfinement: a theoretical-computational study revealing significant enhancement beyond the Langmuirian levels, *Phys. Chem. Chem. Phys.* **2020**, *22*, 19600–19605.

[27] Ramaswamy, R.; González-Segredo, N.; Sbalzarini, I. F.; Grima, R. Discreteness-induced concentration inversion in mesoscopic chemical systems, *Nat. Commun.* **2012**, *3*, 779.

[28] Morimatsu, M.; Takagi, H.; Kosuke G. Ota, R. I.; Yanagida, T.; Sako, Y. Multiple-state reactions between the epidermal growth factor receptor and Grb2 as observed by using single-molecule analysis, *Proc. Natl. Acad. Sci. USA* **2007**, *104*, 18013–18018.

[29] Polarz, S.; Kuschel, A. Chemistry in Confining Reaction Fields with Special Emphasis on Nanoporous Materials, *Chem. Eur. J.* **2008**, *14*, 9816–9829.

[30] Sawada, T.; Yoshizawa, M.; Sato, S.; Fujita, M. Minimal nucleotide duplex formation in water through enclathration in self-assembled hosts, *Nature Chem.* **2009**, *1*, 53–56.

[31] Shon, M. J.; Cohen, A. E. Mass Action at the Single-Molecule Level, *J. Am. Chem. Soc.* **2012**, *134*, 14618–14623.

[32] Patra, S.; Pandey, A. K.; Sarkar, S. K.; Goswami, A. Wonderful nanoconfinement effect on redox reaction equilibrium, *RSC Adv.* **2014**, *4*, 33366–33369.

[33] Patra, S.; Naik, A. N.; Pandey, A. K.; Sen, D.; Mazumder, S.; Goswami, A. Silver nanoparticles stabilized in porous polymer support: A highly active catalytic nanoreactor, *Appl. Catal. A-Gen* **2016**, *524*, 214–222.

[34] Galvin, C. J.; Shirai, K.; Rahmani, A.; Masaya, K.; Shen, A. Q. Total Capture, Convection-Limited Nanofluidic Immunoassays Exhibiting Nanoconfinement Effects, *Anal. Chem.* **2018**, *90*, 3211–3219.

[35] Megarity, C. F.; Siritanaratkul, B.; R. S. Heath, L. W.; Morello, G.; FitzPatrick, S. R.; Booth, R. L.; Sills, A. J.; Robertson, A. W.; Warner, J. H.; Turner, N. J.; Armstrong, F. A. Electrocatalytic Volleyball: Rapid Nanoconfined Nicotinamide Cycling for Organic Synthesis in Electrode Pores, *Angew. Chemie Int. Ed.* **2019**, *58*, 4948–4952.

[36] Downs, A. M.; McCallum, C.; Pennathur, S. Confinement effects on DNA hybridization in electrokinetic micro- and nanofluidic systems, *Electrophoresis* **2019**, *40*, 792–798.

[37] Jonchhe, S.; Pandey, S.; Beneze, C.; Emura, T.; Sugiyama, H.; Endo, M.; Mao, H. Dissection of nanoconfinement and proximity effects on the binding events in DNA origami nanocavity, *Nucleic Acids Res.* **2022**, *50*, 697–703.

[38] Polak, M.; Rubinovich, L. Nanochemical Equilibrium Involving a Small Number of Molecules: A Prediction of a Distinct Confinement Effect, *Nano Lett.* **2008**, *8*, 3543–3547.

[39] Ouldridge, T. E.; Louis, A. A.; Doye, J. P. K. Extracting bulk properties of self-assembling systems from small simulations, *J. Phys.: Condens. Matter* **2010**, *22*, 104102.

[40] Ghosh, K. Stochastic dynamics of complexation reaction in the limit of small numbers, *J. Chem. Phys.* **2011**, *134*, 195101.

[41] Schnell, S. K.; Liu, X.; Simon, J.-M.; Bardow, A.; Bedeaux, D.; Vlugt, T. J. H.; Kjelstrup, S. Calculating Thermodynamic Properties from Fluctuations at Small Scales, *J. Phys. Chem. B* **2011**, *115*, 10911–10918.

[42] De Jong, D. H.; Schäfer, L. V.; De Vries, A. H.; Marrink, S. J.; Berendsen, H. J. C.; Grubmüller, H. Determining Equilibrium Constants for Dimerization Reactions from Molecular Dynamics Simulations, *J. Comp. Chem.* **2011**, *32*, 1919–1928.

[43] Ouldridge, T. E. Inferring bulk self-assembly properties from simulations of small systems with multiple constituent species and small systems in the grand canonical ensemble, *J. Chem. Phys.* **2012**, *137*, 144105.

[44] Polak, M.; Rubinovich, L. The Intrinsic Role of Nanoconfinement in Chemical Equilibrium: Evidence from DNA Hybridization, *Nano Lett.* **2013**, *13*, 2247–2251.

[45] Szymanski, R.; Sosnowski, S.; Maślanka, L. Statistical effects related to low numbers of reacting molecules analyzed for a reversible association reaction A + B = C in ideally dispersed systems: An apparent violation of the law of mass action, *J. Chem. Phys.* **2016**, *144*, 124112.

[46] Cortes-Huerto, R.; Kremer, K.; Potestio, R. Communication: Kirkwood-Buff integrals in the thermodynamic limit from small-sized molecular dynamics simulations, *J. Chem. Phys.* **2016**, *145*, 141103.

[47] Patel, L. A.; Kindt, J. T. Cluster Free Energies from Simple Simulations of Small Numbers of Aggregants: Nucleation of Liquid MTBE from Vapor and Aqueous Phases, *J. Chem. Theory Comput.* **2017**, *13*, 1023–1033.

[48] Zhang, X.; Patel, L. A.; Beckwith, O.; Schneider, R.; Weeden, C. J.; Kindt, J. T. Extracting Aggregation Free Energies of Mixed Clusters from Simulations of Small Systems: Application to Ionic Surfactant Micelles, _J. Chem. Theory Comput._ **2017**, _13_, 5195–5206.

[49] Dawass, N.; Krüger, P.; Schnell, S. K.; Bedeaux, D.; Kjelstrup, S.; Simon, J. M.; Vlugt, T. J. H. Finite-size effects of Kirkwood-Buff integrals from molecular simulations, _Mol. Sim._ **2018**, _44_, 599–612.

[50] Szymanski, R.; Sosnowski, S. Stochasticity of the transfer of reactant molecules between nano-reactors affecting the reversible association A + B ⇌ C, _J. Chem. Phys._ **2019**, _151_, 174113.

[51] Goch, W.; Bal, W. Stochastic or Not? Method To Predict and Quantify the Stochastic Effects on the Association Reaction Equilibria in Nanoscopic Systems, _J. Phys. Chem. A_ **2020**, _124_, 1421–1428.

[52] Lopez, A. J.; Quoika, P. K.; Linke, M.; Hummer, G.; Köfinger, J. Quantifying Protein-Protein Interactions in Molecular Simulations, _J. Phys. Chem. B_ **2020**, _124_, 4673–4685.

[53] Bråten, V.; Wilhelmsen, O.; Schnell, S. K. Chemical Potential Differences in the Macroscopic Limit from Fluctuations in Small Systems, _J. Chem. Inf. Model._ **2021**, _61_, 840–855.

[54] Zangi, R. Binding Reactions at Finite Systems, _Phys. Chem. Chem. Phys._ **2022**, _24_, 9921–9929.

[55] Zangi, R. Statistical Mechanics of Dimerizations and its Consequences for Small Systems, _Phys. Chem. Chem. Phys._ **2022**, _24_, 28804–28813.

[56] Zangi, R. Multimerizations, Aggregation, and Transfer Reactions of Small Numbers of Molecules, _J. Chem. Inf. Model._ **2023**, _63_, 4383–4391.

[57] Rubinovich, L.; Polak, M. Unraveling the Distinct Relationship between the Extent of a Nanoconfined Reaction and the Equilibrium Constant, *J. Phys. Chem. C* **2021**, *125*, 452–457.

[58] Waage, P.; Guldberg, C. M. Studier over Affiniteten, *Forhandlinger i Videnskabs-selskabet i Christiania* **1864**, pages 35–45.

[59] Daniels, F.; Alberty, R. A. *Physical Chemistry;* John Wiley & Sons, Inc.: New York, NY, fourth ed., 1975.

[60] Castellan, G. W. *Physical Chemistry;* Addison-Wesley: Reading, MA, third ed., 1983.

[61] Lebowitz, J. L.; Percus, J. K.; Verlet, L. Ensemble Dependence of Fluctuations with Application to Machine Computations, *Phys. Rev.* **1967**, *153*, 250–254.

[62] McQuarrie, D. A. *Statistical Thermodynamics;* University Science Books: Mill Valley, CA, 1973.

[63] Callen, H. B. *Thermodynamics and an Introduction to Thermostatistics;* John Wiley & Sons: New York, NY, 1985.

[64] Moerner, W. E.; Kador, L. Optical Detection and Spectroscopy of Single Molecules in a Solid, *Phys. Rev. Lett.* **1989**, *62*, 2535–2538.

[65] Brooks Shera, E.; Seitzinger, N. K.; Davis, L. M.; Keller, R. A.; Soper, S. A. Detection of single fluorescent molecules, *Chem. Phys. Lett.* **1990**, *174*, 553–557.

[66] He, M.; Edgar, J. S.; Jeffries, G. D. M.; Lorenz, R. M.; Shelby, J. P.; Chiu, D. T. Selective Encapsulation of Single Cells and Subcellular Organelles into Picoliter- and Femtoliter-Volume Droplets, *Anal. Chem.* **2005**, *77*, 1539–1544.

[67] Reiner, J. E.; Crawford, A. M.; Kishore, R. B.; Goldner, L. S.; Helmerson, K.; Gilson, M. K. Optically trapped aqueous droplets for single molecule studies, *Appl. Phys. Lett.* **2006**, *89*, 013904.

[68] Beer, N. R.; Hindson, B. J.; Wheeler, E. K.; Hall, S. B.; Rose, K. A.; Kennedy, I. M.; Colston, B. W. On-Chip, Real-Time, Single-Copy Polymerase Chain Reaction in Picoliter Droplets, *Anal. Chem.* **2007**, *79*, 8471–8475.

[69] Clausell-Tormos, J.; Lieber, D.; Baret, J.-C.; El-Harrak, A.; Miller, O. J.; Frenz, L.; Blouwolff, J.; Humphry, K. J.; KÃűster, S.; Duan, H.; Holtze, C.; Weitz, D. A.; Griffiths, A. D.; Merten, C. A. Droplet-Based Microfluidic Platforms for the Encapsulation and Screening of Mammalian Cells and Multicellular Organisms, *Chem. Biol.* **2008**, *15*, 427–437.

[70] Rane, T. D.; Puleo, C. M.; Liu, K. J.; Zhang, Y.; Lee, A. P.; Wang, T. H. Counting single molecules in sub-nanolitre droplets, *Lab Chip* **2010**, *10*, 161–164.

[71] Shiomi, H.; Tsuda, S.; Suzuki, H.; Yomo, T. Liposome-Based Liquid Handling Platform Featuring Addition, Mixing, and Aliquoting of Femtoliter Volumes, *PLoS One* **2014**, *9*, 1–6.

[72] Shim, J.-u.; Ranasinghe, R. T.; Smith, C. A.; Ibrahim, S. M.; Hollfelder, F.; Huck, W. T. S.; Klenerman, D.; Abell, C. Ultrarapid Generation of Femtoliter Microfluidic Droplets for Single-Molecule-Counting Immunoassays, *ACS Nano* **2013**, *7*, 5955–5964.

[73] Peters, R. J. R. W.; Marguet, M.; Marais, S.; Fraaije, M. W.; vanâĂĚHest, J. C. M.; Lecommandoux, S. Cascade Reactions in Multicompartmentalized Polymersomes, *Angew. Chemie Int. Ed.* **2014**, *53*, 146–150.

[74] Gahlmann, A.; Ptacin, J. L.; Grover, G.; Quirin, S.; von Diezmann, L.; Lee, M. K.; Backlund, M. P.; Shapiro, L.; Piestun, R.; Moerner, W. E. Quantitative Multicolor Subdiffraction Imaging of Bacterial Protein Ultrastructures in Three Dimensions, *Nano Lett.* **2013**, *13*, 987–993.

[75] Chen, C.; Zong, S.; Wang, Z.; Lu, J.; Zhu, D.; Zhang, Y.; Zhang, R.; Cui, Y. Visualization and intracellular dynamic tracking of exosomes and exosomal miRNAs using single molecule localization microscopy, *Nanoscale* **2018**, *10*, 5154–5162.

[76] Sawant, R. R.; Torchilin, V. P. Liposomes as 'smart' pharmaceutical nanocarriers, *Soft Matter* **2010**, *6*, 4026–4044.

[77] Hsin, T.-M.; Yeung, E. Single-Molecule Reactions in Liposomes, *Angew. Chemie Int. Ed.* **2007**, *46*, 8032–8035.

[78] Cisse, I.; Okumus, B.; Joo, C.; Ha, T. Fueling protein–DNA interactions inside porous nanocontainers, *Proc. Natl. Acad. Sci. USA* **2007**, *104*, 12646–12650.

[79] Lohse, B.; Bolinger, P.-Y.; Stamou, D. Encapsulation Efficiency Measured on Single Small Unilamellar Vesicles, *J. Am. Chem. Soc.* **2008**, *130*, 14372–14373.

[80] Boukobza, E.; Sonnenfeld, A.; Haran, G. Immobilization in Surface-Tethered Lipid Vesicles as a New Tool for Single Biomolecule Spectroscopy, *J. Phys. Chem. B* **2001**, *105*, 12165–12170.

[81] Moonschi, F. H.; Effinger, A. K.; Zhang, X.; Martin, W. E.; Fox, A. M.; Heidary, D. K.; DeRouchey, J. E.; Richards, C. I. Cell-Derived Vesicles for Single-Molecule Imaging of Membrane Proteins, *Angew. Chemie Int. Ed.* **2015**, *54*, 481–484.

[82] Tutkus, M.; Akhtar, P.; Chmeliov, J.; Görföl, F.; Trinkunas, G.; Lambrev, P. H.; Valkunas, L. Fluorescence Microscopy of Single Liposomes with Incorporated Pigment–Proteins, *Langmuir* **2018**, *34*, 14410–14418.

[83] Soga, N.; Ota, A.; Nakajima, K.; Watanabe, R.; Ueno, H.; Noji, H. Monodisperse Liposomes with Femtoliter Volume Enable Quantitative Digital Bioassays of Membrane Transporters and Cell-Free Gene Expression, *ACS Nano* **2020**, *14*, 11700–11711.

[84] Grime, R. L.; Goulding, J.; Uddin, R.; Stoddart, L. A.; Hill, S. J.; Poyner, D. R.; Briddon, S. J.; Wheatley, M. Single molecule binding of a ligand to a G-protein-coupled receptor in real time using fluorescence correlation spectroscopy, rendered possible by nano-encapsulation in styrene maleic acid lipid particles, *Nanoscale* **2020**, *12*, 11518–11525.

[85] Benítez, J. J.; Keller, A. M.; Huffman, D. L.; Yatsunyk, L. A.; Rosenzweig, A. C.; Chen, P. Relating dynamic protein interactions of metallochaperones with metal transfer at the single-molecule level, *Faraday Discuss.* **2011**, *148*, 71–82.

[86] Benítez, J. J.; Keller, A. M.; Ochieng, P.; Yatsunyk, L. A.; Huffman, D. L.; Rosenzweig, A. C.; Chen, P. Probing Transient Copper Chaperone-Wilson Disease Protein Interactions at the Single-Molecule Level with Nanovesicle Trapping, *J. Am. Chem. Soc.* **2008**, *130*, 2446–2447.

[87] Keller, A. M.; Benítez, J. J.; Klarin, D.; Zhong, L.; Goldfogel, M.; Yang, F.; Chen, T.-Y.; Chen, P. Dynamic Multibody Protein Interactions Suggest Versatile Pathways for Copper Trafficking, *J. Am. Chem. Soc.* **2012**, *134*, 8934–8943.

[88] Benítez, J. J.; Keller, A. M.; Ochieng, P.; Yatsunyk, L. A.; Huffman, D. L.; Rosenzweig, A. C.; Chen, P. Probing Transient Copper Chaperone-Wilson Disease Protein Interactions at the Single-Molecule Level with Nanovesicle Trapping, *J. Am. Chem. Soc.* **2009**, *131*, 871–871.

[89] Benítez, J. J.; Keller, A. M.; Chen, P. In *Single Molecule Tools: Fluorescence Based Approaches, Part A*; Walter, N. G., Ed., Vol. 472 of *Meth. Enzymol.;* Academic Press, 2010; pages 41–60.

[90] Allen, M. P.; Tildesley, D. J. *Computer Simulations of Liquids;* Oxford Science Publications: Oxford, 1987.

[91] Frenkel, D.; Smit, B. *Understanding Molecular Simulations: From Algorithms to Applications;* Academic Press: London, 2002.

[92] Metropolis, N.; Rosenbluth, A. W.; Rosenbluth, M. N.; Teller, A. H.; Teller, E. Equation of State Calculations by Fast Computing Machines, *J. Chem. Phys.* **1953**, *21*, 1087–1092.